# Computed Tomographic Analysis of Anterior Clinoid Process Morphology and Pneumatization

M.Sabri Medişoğlu<sup>1</sup>, Melisa Öçbe<sup>2\*</sup>

<sup>1</sup>Kocaeli Health and Technology University, Faculty of Dentistry, Department of Anatomy <sup>2</sup>Kocaeli Health and Technology University, Faculty of Dentistry, Department of Oral and Maxillofacial Radiology

### **ABSTRACT**

The anterior clinoid process (ACP) is a critical anatomical landmark for skull base surgery. Pneumatization of the ACP can affect surgical planning and outcomes. Morphometric evaluation provides essential data for safer interventions.

A total of 154 CT images from individuals aged 1–79 years were retrospectively analyzed. ACP pneumatization types (Type 0–3), bilateral height and width, and inter-ACP distance were evaluated. Morphometric values were stratified by age and gender.

Among 154 patients, 54.5% were female and 45.5% male. Pneumatization was more common in males, with statistically significant differences observed for both left (p < 0.001) and right (p = 0.021) sides. ACP widths showed a moderate positive correlation with age. Males had wider ACPs, whereas females had greater ACP heights. Logistic regression indicated male gender and younger age as predictors of ACP pneumatization.

ACP pneumatization is significantly influenced by gender but not by age. Morphometric differences exist between sexes and age groups. Knowledge of these variations is essential for minimizing intraoperative complications during skull base surgeries.

Keywords: Anterior Clinoid Process, Pneumatization, Computed Tomography, Anatomy, Cross-Sectional

# Introduction

The body of the sphenoid bone is of cartilaginous origin, and its ossification centers are divided into two parts: the presphenoid and the basisphenoid (1,2). The ossification of the posterior clinoid processes (PCPs) begins around the age of 4, and during development, the size of the dorsum sellae increases until puberty (3,4,5). The cranial base can be fundamentally separated into two surfaces: the endocranial surface, which is in contact with nasal cavity, sinuses, orbit, pharynx, infratemporal, and pterygopalatine fossae; and the exocranial surface. These contain numerous foramina, canals, and fissures through which neurological and vascular structures pass. On the intracranial side, the cranial base is divided into anterior, middle, and posterior cranial fossae. The boundary between the anterior and middle fossae formed at the junction of the sulcus chiasmaticus—where the optic chiasm crosses the midline—and the sphenoid crest. The boundary between the middle and posterior cranial fossae is defined by the dorsum sellae, the posterior clinoid processes, and the petrosal ridge. Thus, the central part of the middle cranial base on the endocranial surface is formed by the sphenoid and temporal bones and can be anatomically divided into medial and lateral regions(6). The lateral region includes the greater and lesser wings of the sphenoid bone, and the superior orbital fissure located between them.

The anterior portion of the lesser wing of the sphenoid bone connects to the sphenoid body via a root, forming the roof of the optic canal, while the posterior portion forms the canal's floor and separates the optic canal from the superior orbital fissure. This region is also known as the optic strut (7).

The anterior and posterior clinoid processes (ACPs and PCPs) of the sphenoid bone contribute to the boundaries of the sella turcica. ACP, located at the medial end of the lesser wing, forms the lateral wall of the intracranial end of the optic canal (8). It projects posteriorly from the lesser wing and forms the anterior roof of the cavernous sinus. The base of the ACP has three connection points: the medial edge of the lesser wing, the anterior root of the lesser wing (which forms the roof of the optic canal), and the optic strut (a part

of the lesser sphenoid bone located beneath the optic nerve, forming the canal's floor)(9).

The posterior boundary is formed by a square bony plate known as the dorsum sellae, and the elevation of its superolateral angles gives rise to the posterior clinoid processes (PCPs) (2,10). The PCPs deepen the sella turcica and serve as attachment points for the tentorium cerebelli. The term "clinoid" is derived from the Greek word klineios, meaning "bed-like." The surface of the ACP consists of thick cortical bone, while its inner part is composed of spongy (diploic) bone. However, due to extensive pneumatization of the sphenoid bone, thin-walled, air-filled spaces may form in the ACP through the optic strut. This pneumatization of the ACP results extensions of the paranasal sinuses via the optic strut or anterior root (11). Rupture of these air spaces can result in pneumocephalus cerebrospinal fluid leakage (liquorrhea). Therefore, for surgical interventions in the upper basilar region, the posterior part of the pituitary fossa, the cavernous sinus, and the internal carotid artery, a detailed understanding of the clinoid processes' anatomy is essential (9). The aim of this is to evaluate the anatomy pneumatization patterns in computed tomography (CT) images, retrospectively.

### Materials and Methods

This retrospective study was approved by the Non-invasive Clinical Research Ethics Committee of Kocaeli Health and Technology University on April 21, 2025 (Project No: 2025-161) and conducted in accordance with the Declaration of Helsinki. The Institutional Review Board reviewed and approved the protocol, and all patient data were anonymized to ensure confidentiality. CT scans of the anterior clinoid process from 1783 patients, obtained between 2022 and March 2024 at the Department of Radiology, Kocaeli City Hospital, were retrospectively reviewed. Inclusion criteria were age ≥1 year, high-quality diagnostic images, and absence of sphenoid bone, sphenoid sinus, or sella turcica pathology. Exclusion criteria included emergency cases and prior cranial surgery.

All scans were acquired using the Revolution<sup>TM</sup> EVO/Optima<sup>TM</sup> CT660 system (GE Healthcare Japan, Tokyo, Japan) with standardized parameters: 120 kVp, auto mA (100–250 mA), 0.625-mm slice thickness, 0.5-mm reconstruction interval, 250-mm FOV, Bone Plus Kernel, and a 512 × 512 matrix. Patients were scanned supine

with the Frankfort horizontal plane perpendicular to the table. Images with motion or metallic artifacts were excluded. Multiplanar reformation (axial, coronal, sagittal) was performed. Two independent reviewers—one oral and maxillofacial radiologist and one anatomy specialist—evaluated all scans using a dedicated workstation under standardized viewing conditions.

The pneumatization degrees of ACP were classified according to the study of Abuzadey et al. (2010) as following; Type 0 non pneumatized ACP, Type I less than 50% pneumatization of the ACP, Type II more than 50% pneumatization (without total pneumatization), and Type III total pneumatization of ACP. Pneumatization status was assessed in axial and coronal planes, primarily by identifying air density regions (hypodense areas consistent with pneumatized air cells) within the anterior clinoid process. The optic strut, a bony structure between the body of the sphenoid and ACP, and the sphenoid sinus boundaries were used as critical anatomical references for classification. (See Figure 1 for examples of each type.) (Figure 1)

In addition to the pneumatization assessment, morphometric measurements were obtained using standardized anatomical landmarks. The distance between the anterior and posterior clinoid processes was measured on axial CT images as the linear span between the medial tip of the ACP and the medial tip of the posterior clinoid process, which lies on the dorsum sellae. measurement helped to estimate the clinoid span and evaluate variations in the sella turcica region related with age and gender (Figure 2).

The height and width of the ACP were measured bilaterally on coronal CT images. ACP height was defined as the vertical distance from the inferior margin of the ACP, at its junction with the sphenoid body, to its most superior point. This measurement was obtained by referencing the region between the superior orbital fissure inferiorly and the roof of the optic canal superiorly. The ACP width was determined as the maximum transverse dimension of the process at its midpoint, extending from its medial to lateral border. This was measured in a coronal plane approximately midway between the optic strut and the roof of the optic canal (Figure 2).

All morphometric values were recorded in millimeters. Images with significant motion artifacts, anatomical distortion, or incomplete visibility of the relevant landmarks were excluded from the study. Statistical Analysis: All statistical analyses were conducted using IBM SPSS Statistics for Windows, Version 25.0 (IBM Corp., Armonk, NY, USA). Descriptive statistics were calculated for each morphological parameter of the anterior clinoid process (ACP), including minimum, maximum, mean, and standard deviation (SD). The distribution of categorical variables, such as gender and ACP pneumatization types, was summarized using frequencies and percentages. Normality was assessed using the Shapiro-Wilk test. Independent-samples t-tests were used to compare continuous ACP measurements between male and female participants. One-way ANOVA with post-hoc analysis was performed to evaluate differences in ACP measurements across age groups.

Pearson's correlation coefficient was used to examine the relationship between age and continuous ACP measurements for the entire sample, as well as stratified by gender. For nonparametric data, including ordinal pneumatization scores, Spearman's rank correlation coefficient (o) was calculated to assess associations with age. To evaluate associations between categorical variables such as gender and ACP pneumatization types, Chi-square  $(\chi^2)$  tests were applied. Additionally, binary logistic regression models were constructed separately for left and right ACP pneumatization to assess the predictive value of age and gender. Regression coefficients, p-values, and pseudo Rsquared values (Nagelkerke R2) were reported to assess model fit and variable significance. A pvalue of <0.05 was considered statistically significant.

## Results

**Descriptive Statistics:** A total of 154 patients were included in this study, comprising 84 females (54.55%) and 70 males (45.45%), with a mean age of 23.25  $\pm$  18.11 years (range: 1 to 79 years). Descriptive analysis of anterior clinoid process (ACP) measurements revealed the following mean values: distance between the ACPs was 25.97  $\pm$  5.50 mm (range: 9.70–43.55 mm), right ACP height was 11.21  $\pm$  3.08 mm (range: 5.50–17.09 mm), right ACP width was 5.06  $\pm$  1.59 mm (range: 2.48–9.49 mm), left ACP height was 11.78  $\pm$  4.34 mm (range: 4.68–29.38 mm), and left ACP width was 5.69  $\pm$  1.61 mm (range: 3.21–9.83 mm) (Table 1).

ACP Measurements by Gender: Gender-based comparisons showed that males had a higher mean distance between ACPs ( $26.72 \pm 6.05$  mm) than

females (25.34  $\pm$  4.94 mm). However, females exhibited greater right ACP height (11.88  $\pm$  3.13 mm vs. 10.41  $\pm$  2.85 mm) and left ACP height (12.01  $\pm$  3.31 mm vs. 11.52  $\pm$  5.34 mm). In contrast, ACP widths were greater in males: right ACP width averaged 5.46  $\pm$  1.86 mm in males vs. 4.73  $\pm$  1.24 mm in females; left ACP width was 6.11  $\pm$  1.60 mm in males vs. 5.34  $\pm$  1.55 mm in females (Table 2) (Figure 3).

Age Group Distribution: Participants were stratified into five age groups: 44 patients (28.57%) were children (0–12 years), 54 (35.06%) were teenagers (13-19 years), 24 (15.58%) were young adults (20-39 years), 24 (15.58%) were middle-aged adults (40-59 years), and 8 (5.19%) were older adults (60+ years). Gender distribution across age groups was balanced, with no statistically significant association between gender and age group ( $\chi^2 = 3.42$ , df = 4, p = 0.491). Specifically, among children, 54.55% were female and 45.45% male; among teenagers, 62.96% were female and 37.04% male; among young adults, 41.67% were female and 58.33% male; among middle-aged adults, 50.00% were female and male each; and among older adults, 50.00% were female and male each.

ACP Measurements by Age Group: Age group-based analysis revealed trends in ACP morphology. In children (0–12 years), the mean distance between ACPs was 25.09  $\pm$  5.82 mm, with right height 10.35  $\pm$  2.98 mm, right width 4.89  $\pm$  1.78 mm, left height 12.21  $\pm$  6.35 mm, and left width 5.18  $\pm$  1.30 mm. Teenagers (13–19 years) had a slightly increased mean distance of 25.68  $\pm$  7.06 mm, with right height 11.71  $\pm$  2.72 mm, right width 4.60  $\pm$  1.27 mm, left height 12.92  $\pm$  3.22 mm, and left width 5.22  $\pm$  1.26 mm (Table 3).

In young adults (20–39 years), the distance increased to 27.12  $\pm$  2.89 mm, right height was  $10.55 \pm 2.02$  mm, right width  $4.97 \pm 1.22$  mm, left height  $10.06 \pm 2.05$  mm, and left width  $6.18 \pm 1.84$  mm. Middle-aged adults (40–59 years) exhibited further increase in width, with mean right ACP width of  $6.50 \pm 1.60$  mm and left ACP width of  $7.06 \pm 1.95$  mm, along with a right height of  $13.59 \pm 3.39$  mm, left height of  $11.23 \pm 3.12$  mm, and distance of  $26.81 \pm 3.24$  mm. In older adults (60–79 years), the measurements were more stable: distance between ACPs was  $26.73 \pm 0.26$  mm, right height  $7.41 \pm 1.45$  mm, right width  $5.03 \pm 1.22$  mm, left height  $8.60 \pm 2.56$  mm, and left width  $6.05 \pm 0.45$  mm (Table 3) (Figure 4, 5).

Correlation Analysis: Pearson correlation analysis showed a moderate positive correlation between

**Table 1:** Descriptive Statistics of ACP Measurements

Measurement	Minimum (mm)	Maximum (mm)	Mean (mm)	SD (mm)
Distance between right and left ACP	9.70	43.55	25.97	5.50
Right ACP Height	5.50	17.09	11.21	3.08
Right ACP Width	2.48	9.49	5.06	1.59
Left ACP Height	4.68	29.38	11.78	4.34
Left ACP Width	3.21	9.83	5.69	1.61

Table 2: ACP Measurements Stratified by Gender

Measurement	Female (Mean ± SD)	Male (Mean ± SD)
Distance between right and left ACP	$25.34 \pm 4.94$	$26.72 \pm 6.05$
Right ACP Height	$11.88 \pm 3.13$	$10.41 \pm 2.85$
Right ACP Width	$4.73 \pm 1.24$	$5.46 \pm 1.86$
Left ACP Height	$12.01 \pm 3.31$	$11.52 \pm 5.34$
Left ACP Width	$5.34 \pm 1.55$	6.11 ± 1.60

Table 3: ACP Measurements by Age Group

Age Group	Distance Between Right and Left ACP (Mean ± SD)	Right ACP Height	Right ACP Width	Left ACP Height	Left ACP Width
Children (0– 12)	$25.09 \pm 5.82$	$10.35 \pm 2.98$	$4.89 \pm 1.78$	$12.21 \pm 6.35$	5.18 ± 1.30
Teenagers (13–19)	$25.68 \pm 7.06$	11.71 ± 2.72	$4.60 \pm 1.27$	$12.92 \pm 3.22$	$5.22 \pm 1.26$
Young Adults (20–39)	$27.12 \pm 2.89$	$10.55 \pm 2.02$	$4.97 \pm 1.22$	$10.06 \pm 2.05$	$6.18 \pm 1.84$
Middle-aged (40–59)	$26.81 \pm 3.24$	$13.59 \pm 3.39$	$6.50 \pm 1.60$	$11.23 \pm 3.12$	$7.06 \pm 1.95$
Older Adults (60–79)	$26.73 \pm 0.26$	7.41 ± 1.45	$5.03 \pm 1.22$	$8.60 \pm 2.56$	$6.05 \pm 0.45$

Table 4: Pearson Correlation Between Age and ACP Measurements (Stratified by Gender)

Measurement	Total (r)	Female (r, p)	Male (r, p)
Distance between right and left ACP	0.134	0.092, p = 0.404	0.158, p = 0.191
Right ACP Height	0.102	-0.043, p = 0.699	0.299, p = 0.012
Right ACP Width	0.284	0.210, p = 0.055	0.331, p = 0.005
Left ACP Height	-0.186	-0.284, p = $0.009$	-0.122, p = $0.313$
Left ACP Width	0.315	0.277, p = 0.011	0.347, p = 0.003

age and ACP widths - right width (r = 0.284) and left width (r = 0.315). No meaningful correlation was observed between age and distance between ACPs (r = 0.134), right height (r = 0.102), or left height (r = -0.186) (Table 4).

Females showed a significant negative correlation between age and left ACP height (r = -0.284, p = 0.009) and a significant positive correlation with left ACP width (r = 0.277, p = 0.011). Right ACP width showed borderline significance (r = 0.210, p = 0.055), while other parameters were not

Table 5: Distribution of ACP Pneumatization Types by Gender

Side	Pneumatization Type	Female (n, %)	Male (n, %)
Left	Type 0	78 (92.86%)	46 (65.71%)
	Type 1	0 (0.00%)	12 (17.14%)
	Type 2	1 (1.19%)	2 (2.86%)
	Type 3	6 (7.14%)	12 (17.14%)
Right	Type 0	74 (88.10%)	50 (71.43%)
	Type 1	4 (4.76%)	12 (17.14%)
	Type 2	1 (1.19%)	3 (4.29%)
	Type 3	6 (7.14%)	8 (11.43%)

Table 6: Chi-square Test Results for Pneumatization vs. Gender

Side	χ² Value	df	p-value	Interpretation
Left	21.16	2	< 0.001	Significant association
Right	7.72	2	0.021	Significant association

Table 7: Binary Logistic Regression Predicting ACP Pneumatization

	Predictor	Coefficient (β)	p-value	Odds Ratio (e^β)	Interpretation
Left	Age	-0.0425	0.009	0.958	Younger age = higher risk
	Gender (Male)	2.04	< 0.001	7.69	Males = significantly higher likelihood
	Model p-value	_	< 0.000001	_	Model is highly significant
	Pseudo R²	_	_	_	0.183
Right	Age	-0.0287	0.043	0.972	Younger age = higher risk
	Gender (Male)	1.15	0.008	3.16	Males = significantly higher likelihood
	Model p-value	_	0.0029	_	Model is statistically significant
	Pseudo R²	_	_	_	0.077

significantly correlated. Males demonstrated a positive correlation between age and ACP right height (r = 0.299, p = 0.012), right width (r = 0.331, p = 0.005), and left width (r = 0.347, p = 0.003). No significant correlations were found with distance (r = 0.158, p = 0.191) or left height (r = -0.122, p = 0.313) (Table 4).

ACP Pneumatization: ACP pneumatization was evaluated separately for the left and right sides. On the left side, pneumatization was absent (type 0) in 124 cases (80.52%), type 1 in 9 cases (5.84%), type 2 in 3 cases (1.95%) and type 3 in 18 cases (11.69%). On the right side, type 0 was observed in 124 cases (80.52%), type 1 in 12 cases (7.79%), type 2 in 4 cases (2.6%) and type 3 in 14 cases (9.09%) (Table 5). Spearman correlation analysis indicated no statistically significant

association between age and pneumatization on either side (left:  $\varrho$  = -0.115, p = 0.154; right:  $\varrho$  = -0.059, p = 0.466). However, chi-square analysis revealed significant associations between gender and ACP pneumatization: on the left side,  $\chi^2$  = 21.16, p < 0.001; on the right side,  $\chi^2$  = 7.72, p = 0.021. Gender-stratified pneumatization patterns demonstrated that males had significantly higher rates of pneumatization, especially for advanced types (Table 6) (Figure 3).

**Logistic Regression Analysis:** Binary logistic regression was performed to determine predictors of ACP pneumatization:

For left-side pneumatization, age was a significant negative predictor (coefficient = -0.0425, p = 0.009), and male gender (coded as 2) was a strong positive predictor (coefficient = 2.04, p < 0.001).

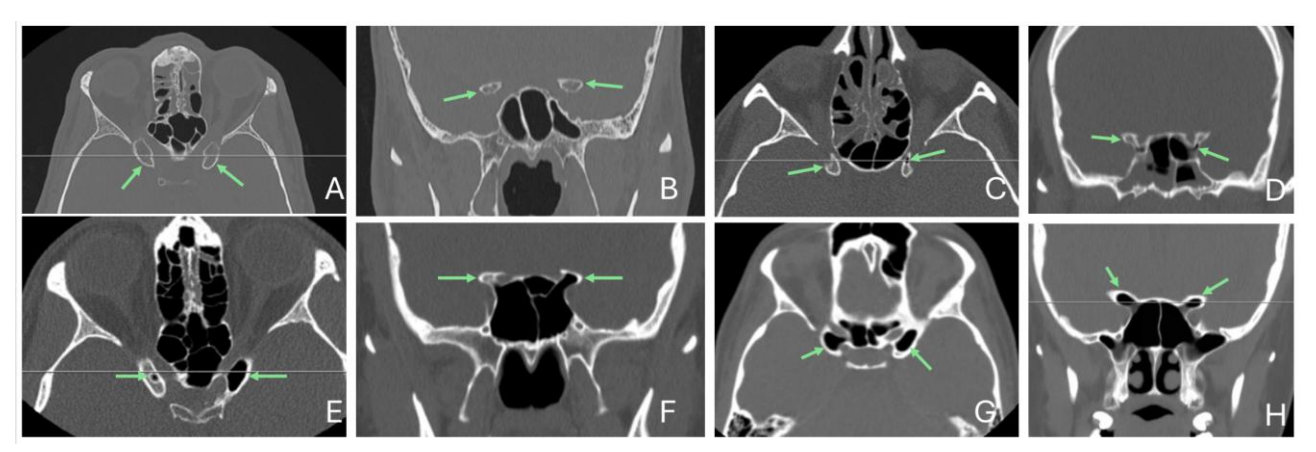


**Fig. 1.** Representative CT images illustrating the types of anterior clinoid process (ACP) pneumatization. A and B: Axial and coronal CT sections demonstrating Type 0 ACP pneumatization bilaterally. C and D: Axial and coronal sections of a patient with Type 1 pneumatization on the right side (arrow) and Type 0 on the left. E and F: Axial and coronal sections of another patient showing Type 1 ACP pneumatization on the right and Type 2 on the left. G and H: Axial and coronal sections depicting bilateral Type 3 ACP pneumatization

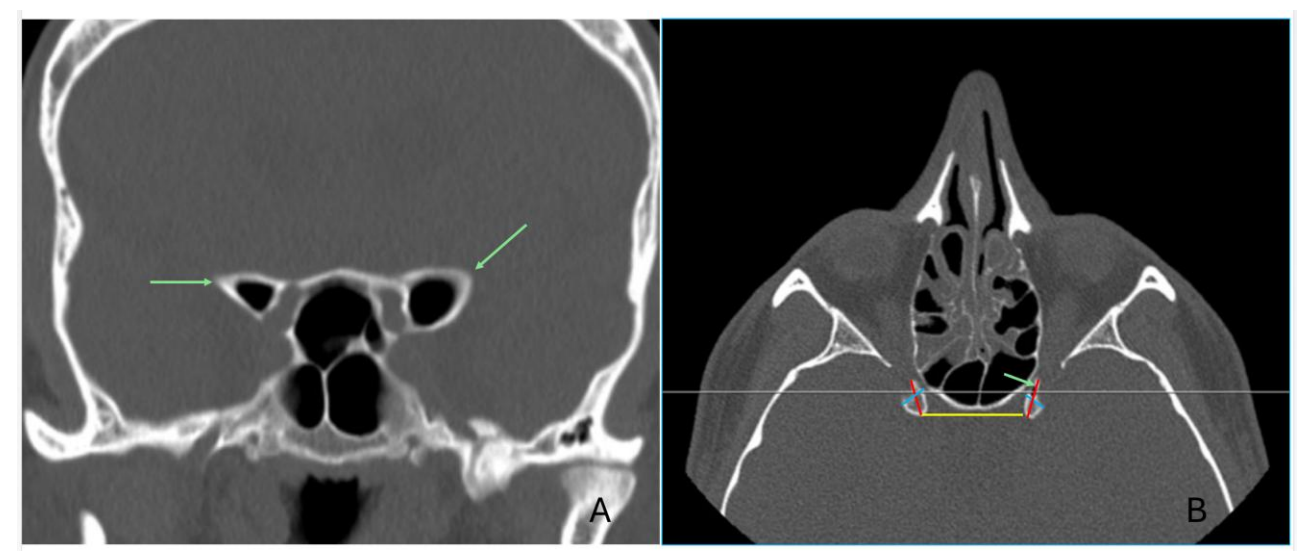


Fig. 2. Coronal (A) and axial (B) computed tomography (CT) images of the anterior clinoid process (ACP). Panel B also illustrates the morphological measurements of the ACP: the yellow line indicates the distance between themedial tips of the right and left ACPs, the red line represents ACP height, defined as the vertical distance from the inferiormargin of the ACP at its junction with the sphenoid body to itsmost superior point, the blue line represents ACP width, defined as the maximum transverse dimension from themedial to the lateral border of the ACP at its midpoint, measured in the coronal plane

The model was statistically significant (p < 0.000001) with a Pseudo R<sup>2</sup> of 0.183.

For right-side pneumatization, age also showed a negative association (coefficient = -0.0287, p = 0.043), while male gender remained a significant positive predictor (coefficient = 1.15, p = 0.008). The model had a significance level of p = 0.0029 and Pseudo R<sup>2</sup> of 0.077 (Table 7).

# Discussion

The anatomical structure of the ACP and its relationship with the vital neurovascular structures

in the region is critically important in skull base surgery. The ACP is covered by dense cortical is formed bone and primarily bv anterosuperior portion of the lesser wing of the sphenoid bone and the posteroinferior optic strut (8,11,12). Since the internal carotid artery (ICA) lies close to the medial and inferior parts of the ACP, surgical intervention for lesions adjacent to or involving the ACP typically requires an anterior clinoidectomy via an anterior approach. This approach has long been considered the gold standard for such pathologies (13-16). Therefore, preoperative evaluation of the ACP

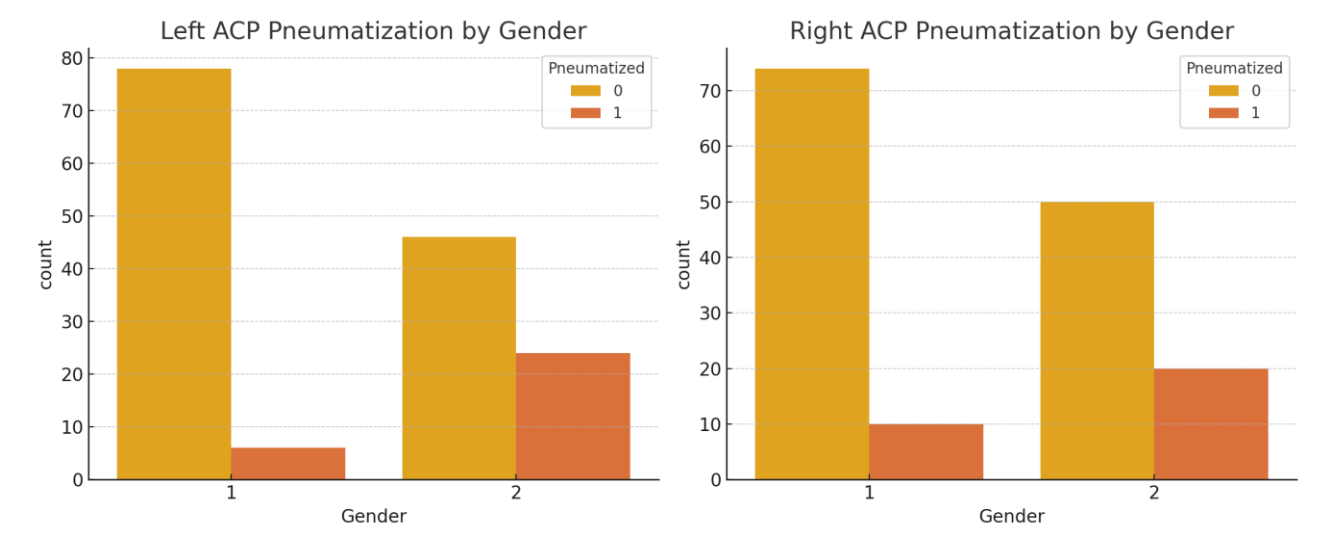


**Fig. 3.** Graphical presentation of left and right anterior clinoid process (ACP) pneumatization presence in both genders. Males were found to be significantly more likely to show pneumatization on the left and right sides

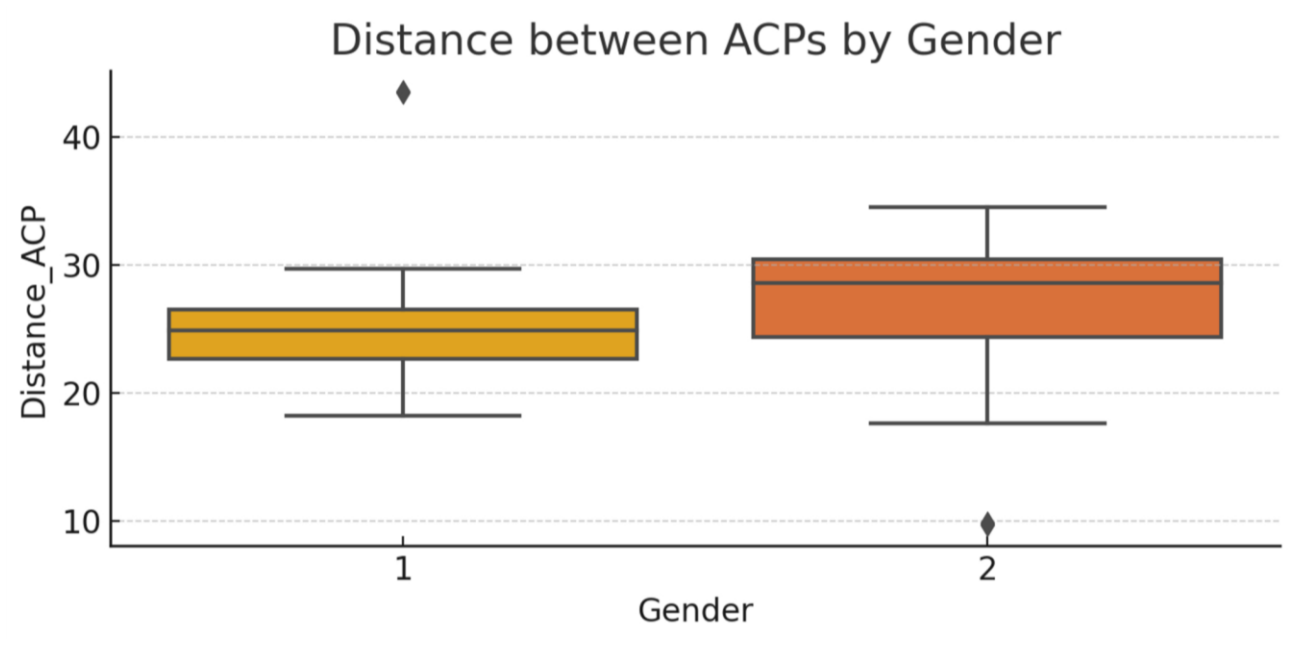


Fig. 4. Comparison of the distance between anterior clinoid processes (ACPs) by gender. While both males and females demonstrate overlapping ranges, males exhibit a slightly broader distribution

recommended by clinical practitioners to enable safer and more efficient high-speed surgical interventions (11,17).

In pneumatized ACPs, the likelihood of intraoperative damage to neurovascular structures may be increased compared to non-pneumatized and fully osseous structures. This has been attributed to high-power drilling instruments coming into forceful contact with the thin-walled, air-filled bone, potentially damaging surrounding critical structures such as the cerebral cortex, cranial nerves, ICA, orbital contents, or cavernous sinus (13,18).

ACP is fundamentally an osseous structure. The incidence of pneumatized ACPs has been reported to range from 4% to 29.3% in various studies (11,19-23). Based on these findings, it can be inferred that approximately one-third of ACPs are pneumatized. In our study, pneumatization types were evaluated bilaterally and in relation to sex. Among females, the right and left non-pneumatized ACPs were found in 88.1% and 92.8% of cases, respectively. In males, the respective values were 71.4% and 65.7%. These findings are consistent with the ranges reported in the literature. Notably, the prevalence of

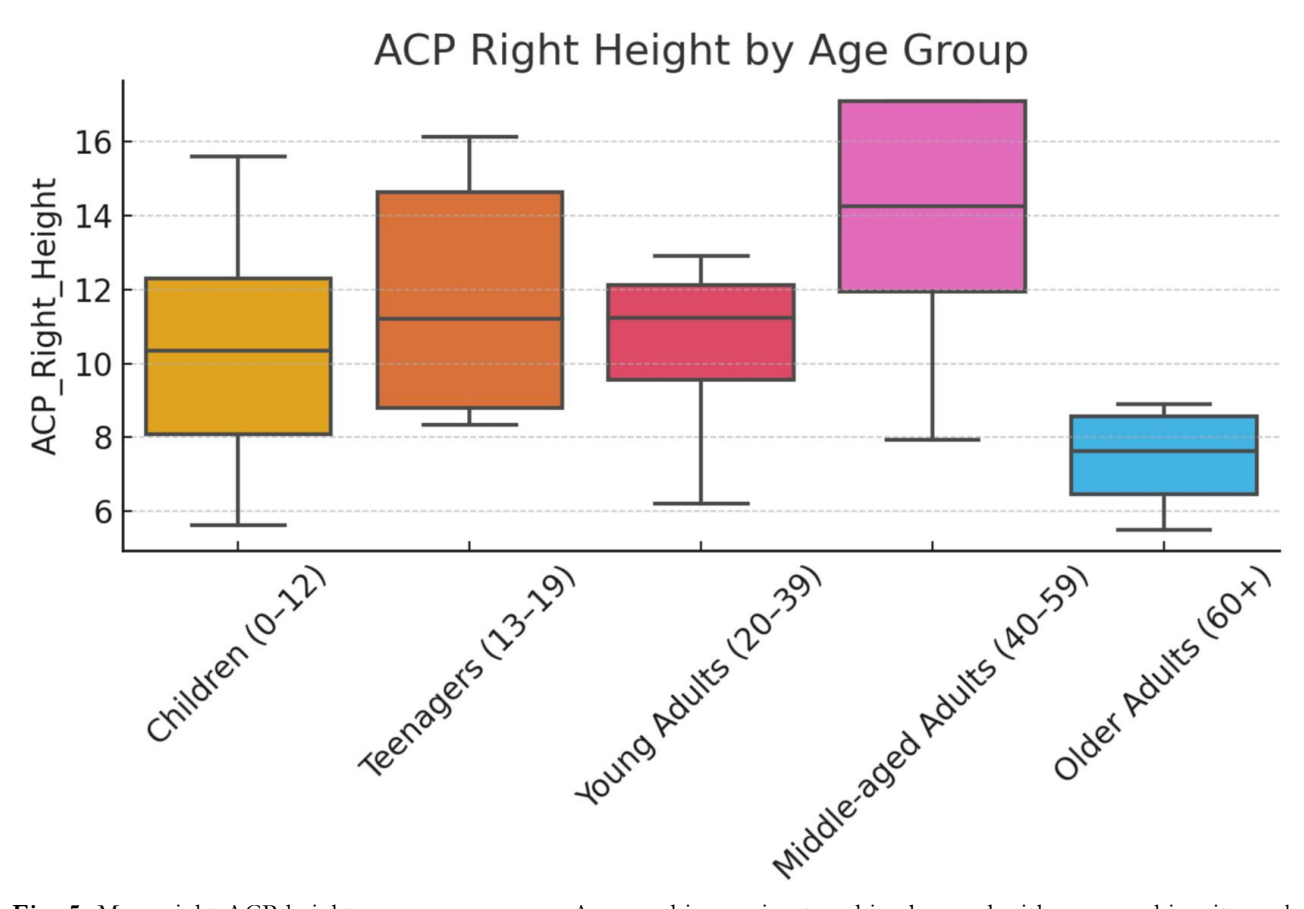


Fig. 5. Mean right ACP height across age groups. A general increasing trend is observed with age, reaching its peak in middle-aged adults

pneumatization (types 1 and 3) was significantly higher in males (right: 33%, left: 37%) compared to females (right: 13%, left: 8%), indicating a clear sex-based difference. This contrasts with some studies that reported no sex-related differences in ACP pneumatization (11,21). While some authors have suggested that ACP pneumatization may facilitate surgical access (11), others argue it may actually increase surgical risk (24). Our findings support the latter view. In our study, no direct association was found between ageand ACP pneumatization in the correlation analysis, whereaslogistic regression analysis identified younger age as a significant predictor. This discrepancy may be explained bythe fact that the effect of age becomes more apparent when theinfluence of gender is controlled. Therefore, although agealone does not appear to be a decisive factor, it plays a role in pneumatization when evaluated together with gender.

In this study, ACP height and width were also measured in relation to sex. Among females, the right and left heights were 11.88  $\pm$  3.13 mm and 12.01  $\pm$  3.31 mm, and the right and left widths were 4.73  $\pm$  1.24 mm and 5.34  $\pm$  1.55 mm,

respectively. Among males, the right and left heights were 10.41  $\pm$  2.85 mm and 11.52  $\pm$  5.34 mm, and the right and left widths were 5.46  $\pm$ 1.86 mm and 6.11  $\pm$  1.60 mm. In a study by Gupta et al., the mean lengths of the ACP on the right and left sides were reported as  $11.1 \pm 1.49$ mm and  $11.61 \pm 2.07$  mm, respectively (25). In contrast, a study by Lee et al. on a Korean population reported shorter lengths of 9.26  $\pm$  1.43 mm and  $9.09 \pm 1.67$  mm for the right and left ACPs, respectively [26]. Another study by Gupta et al. conducted on a Nepalese population found right and left lengths of  $10.74 \pm 2.37$  mm and 9.91± 1.50 mm, respectively (25). Kapur et al. reported average ACP lengths in males as 9.9 ± 1.6 mm (right) and 9.3  $\pm$  1.4 mm (left), and in females as  $9.3 \pm 1.6$  mm (right) and  $8.9 \pm 2.0$  mm (left) (17). D'Souza et al. reported longer average lengths and widths, with male ACP lengths of 12.07 mm (right) and 12.46 mm (left), and female lengths of 12.21 mm (right) and 12.28 mm (left); widths were 10.30 mm (right) and 11.23 mm (left) in males, and 10.64 mm (right) and 11.35 mm (left) in females (27).

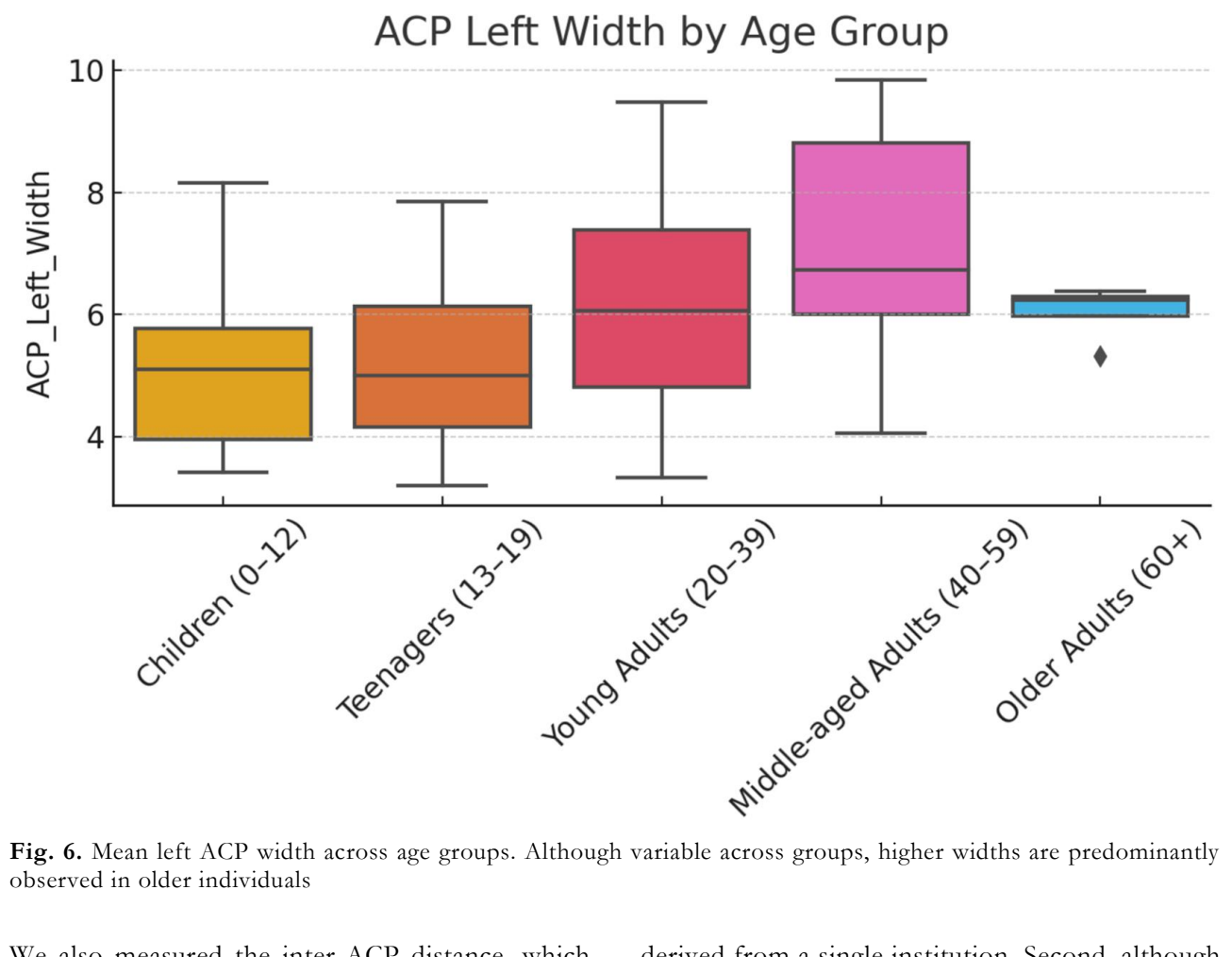


Fig. 6. Mean left ACP width across age groups. Although variable across groups, higher widths are predominantly observed in older individuals

We also measured the inter-ACP distance, which was found to be 25.34 ± 4.94 mm in females and 26.72 ± 6.05 mm in males. Ertürk et al. reported this distance as 22.6 mm (28), while another study reported a value of 25.8 mm (29). Compared to previous studies, our measurements appear larger than those by Gupta, Kapur, and Lee, but slightly smaller than those by D'Souza et al. These differences may stem from variations in measurement techniques and in the precise identification of bony landmarks. Additionally, racial and ethnic differences in cranial morphology must also be considered. From this perspective, the values obtained in our study are broadly consistent with the literature.

A comprehensive understanding of the regional anatomy has enabled advancements in skull base, including the development of microsurgical techniques and new diagnostic approaches. These advances have allowed for the implementation of more radical surgical interventions while reducing the risk of neurovascular injury during procedures (30-32).

Limitations: This study has several limitations that should be considered. First, the sample was derived from a single institution. Second, although high-resolution CT images were used, assessment of pneumatization morphometric measurements may still involve a degree of observer subjectivity. Third, the crosssectional design does not allow for evaluation of anatomical changes over time, particularly across Additionally, different age groups. developmental or pathological conditions that could influence ACP morphology (such as endocrinological disorders craniofacial or anomalies) were not systematically excluded. In addition, although we included participants across a wide age range, the cohort was predominantly young (mean age 23.2 ± 18.1 years) with only 5.2% aged ≥60 years. This imbalance limits the strength of age-related analyses and may underrepresent anatomical variations that emerge in older adults.

the surgical and importance of ACP morphology, this study aimed to emphasize the detailed morphometry of the structure, to investigate its relationship with age and sex, and to examine its anatomical relations to surrounding structures to provide clinically

relevant data for safe and precise surgical interventions. Our findings revealed the need for comprehensive preoperative CT evaluation of the anterior clinoid process, particularly in male and younger patients who show higher pneumatization rates. Recognizing these anatomic variants allows skull-base surgeons to modify drilling strategies and reduce the risk of optic nerve or internal carotid artery injury during anterior clinoidectomy interventions. related Α thorough understanding of this region's anatomy is not only crucial for improved surgical access but also necessary for developing techniques that minimize the risk of injury to associated neurovascular structures.

### References

- 1. Tubbs RS, Salter EG, Oakes WJ. Quantitation of and measurements utilizing the sphenoid ridge. Clin Anat 2007; 20: 131-134.
- 2. Arey LB. Developmental anatomy. 7th ed. Philadelphia: W.B. Saunders Co; 1965. p. 306.
- 3. Tang CT, Baidya NB, Tseng KY, Ma HI. Posterior clinoid process as a landmarker in current endoscopic-assisted neurosurgical approaches. Formos J Surg 2012; 45: 45-50.
- 4. Gordon MB, Bell AL. A roentgenographic study of the sella turcica in normal children. N Y State J Med 1922; 22: 54-59.
- 5. Berger PE, Harwood-Nash DC, Fitz CR. The dorsum sella in infancy and childhood. Pediatr Radiol 1976; 4: 214-220.
- 6. Rhoton AL Jr. The anterior and middle cranial base. Neurosurgery 2002; 51: 273-302.
- 7. Natori Y, Rhoton AL Jr. Microsurgical anatomy of the superior orbital fissure. Neurosurgery 1995; 36: 762-775.
- 8. Inoue T, Rhoton AL Jr, Theele D, Barry ME. Surgical approaches to the cavernous sinus: a microsurgical study. Neurosurgery 1990; 26: 903-932.
- 9. Burulday V, Akgül MH, Ozveren MF, Kaya A. Evaluation of posterior clinoid process pneumatization by multidetector computed tomography. Neurosurg Rev 2017; 40: 403-409.
- 10. Standring S, Ellis H, Berkovitz BKB, et al., editors. Gray's Anatomy: The Anatomical Basis of Clinical Practice. 39th ed. New York: Elsevier Churchill Livingstone; 2005. p. 462.
- 11. Abuzayed B, Tanriover N, Biceroglu H, et al. Pneumatization degree of the anterior clinoid process: a new classification. Neurosurg Rev 2010; 33: 367-374.
- 12. Kim JH, Kim JM, Cheong JH, et al. Simple anterior petroclinoid fold resection in the

- treatment of low-lying internal carotid-posterior communicating artery aneurysms. Surg Neurol 2009; 72: 142-145.
- Chang DJ. The "no-drill" technique of anterior clinoidectomy: a cranial base approach to the paraclinoid and parasellar region. Neurosurgery 2009; 64: ONS96-ONS105.
- 14. Dolenc VV. A combined epi- and subdural direct approach to carotid-ophthalmic artery aneurysms. J Neurosurg 1985; 62: 667-672.
- 15. Noguchi A, Balasingam V, Shiokawa Y, et al. Extradural anterior clinoidectomy. Technical note. J Neurosurg 2005; 102: 945-950.
- 16. Nutik SL. Removal of the anterior clinoid process for exposure of the proximal intracranial carotid artery. J Neurosurg 1988; 69: 529-553.
- 17. Kapur E, Mehic A. Anatomical variations and morphometric study of the optic strut and the anterior clinoid process. Bosn J Basic Med Sci 2012; 12: 88-93.
- 18. Son HE, Park MS, Kim SM, et al. The avoidance of microsurgical complications in the extradural anterior clinoidectomy to paraclinoid aneurysms. J Korean Neurosurg Soc 2010; 48: 199-206.
- 19. Citardi MJ, Gallivan RP, Batra PS, et al. Quantitative computer-aided computed tomography analysis of sphenoid sinus anatomical relationships. Am J Rhinol 2004; 18: 173-178.
- 20. DeLano MC, Fun FY, Zinreich SJ. Relationship of the optic nerve to the posterior paranasal sinuses: a CT anatomic study. Am J Neuroradiol 1996; 17: 669-675.
- 21. Mikami T, Minamida Y, Koyanagi I, et al. Anatomical variations in pneumatization of the anterior clinoid process. J Neurosurg 2007; 106: 170-174.
- 22. Sapci T, Derin E, Almac S, et al. The relationship between the sphenoid and the posterior ethmoid sinuses and the optic nerves in Turkish patients. Rhinology 2004; 42: 30-34
- 23. Sirikci A, Bayazit YA, Bayram M, et al. Variations of sphenoid and related structures. Eur Radiol 2000; 10: 844-848.
- 24. Szumada T, Sloniewski P, Baczalska A, et al. The pneumatisation of anterior clinoid process is not associated with any predictors that might be recognised preoperatively. Folia Morphol (Warsz) 2013; 72: 100-106.
- 25. Gupta N, Ray B, Ghosh S. A study on anterior clinoid process and optic strut with emphasis on variations of caroticoclinoid foramen. Nepal Med Coll J 2005; 7: 141-144.

- 26. Lee HY, Chung IH, Choi BY, et al. Anterior clinoid process and optic strut in Koreans. Yonsei Med J 1997; 38: 151-154.
- 27. D'Souza A, Ankolekar VH, Nayak N, et al. Morphometric study of anterior clinoid process and optic strut and the ossification of carotico-clinoid ligament with their clinical importance. J Clin Diagn Res 2016; 10: AC05-07.
- 28. Erturk M, Kayalioglu G, Govsa F. Anatomy of the clinoidal region with special emphasis on the caroticoclinoid foramen and interclinoid osseous bridge in a recent Turkish population. Neurosurg Rev 2004; 27: 22-26.
- 29. Boyan N, Ozsahin E, Kizilkanat E, et al. Surgical importance of the morphometry of the anterior clinoid process, optic strut,

- caroticoclinoid foramen, and interclinoid osseous bridge. Neurosurg Q 2011; 21: 133.
- 30. Huynh-Le P, Natori Y, Sasaki T. Surgical anatomy of the ophthalmic artery: its origin and proximal course. Neurosurgery 2005; 57: 236-241.
- 31. Hayashi N, Masuoka T, Tomita T, et al. Surgical anatomy and efficient modification of procedures for selective extradural anterior clinoidectomy. Minim Invasive Neurosurg 2004; 47: 355-358.
- 32. Puzzilli F, Ruggeri A, Mastronardi L, et al. Anterior clinoidal meningiomas: report of a series of 33 patients operated on through the pterional approach. Neuro Oncol 1999; 1: 188-195.

East J Med Volume:30, Number:4, October-December/2025